

Patterning of hydrogen-passivated Si(100) using Ar($^3P_{0,2}$) metastable atoms

S. B. Hill, C. A. Haich, F. B. Dunning and G. K. Walters

Department of Physics and the Rice Quantum Institute, Rice University

P. O. Box 1892, Houston, TX 77251-1892

J. J. McClelland, R. J. Celotta

Electron Physics Group, National Institute of Standards and Technology

Gaithersburg, MD 20899

H. G. Craighead

School of Applied and Engineering Physics, Cornell University

Ithaca, NY 14853

ABSTRACT

We describe the patterning of silicon by exposing a hydrogen-passivated Si(100) surface to Ar($^3P_{0,2}$) metastable atoms through a fine Ni grid in the presence of a small background pressure of oxygen is described. Metastable atom impact leads to the formation of a uniform oxide layer that is sufficiently resistant to chemical etching to allow feature depths $\gtrsim 20$ nm to be realized. With optical manipulation of the incident metastable atoms, this technique could provide the basis for massively-parallel nanoscale fabrication on silicon without the use of organic resists.

PACS numbers: 81.65.C, 85.40.Hp, 85.40.Ux, 79.20.Rf

Much recent effort has centered on developing nanolithography techniques for patterning silicon surfaces. The goal of this work is to modify localized surface regions so they become resistant or susceptible to subsequent etching. A variety of approaches have been examined ranging from those that rely on optical exposure through a mask¹⁻³ to those that make use of high energy electron beams⁴, scanning tunneling microscopy⁵⁻⁷ or atomic force microscopy⁸⁻¹⁰ to directly write patterns on a surface. Neutral metastable atoms can also be used to modify surfaces and are particularly attractive for use in patterning because the resolution that they provide is not limited by diffraction effects, by secondary electron scattering or by electrostatic interactions.¹¹ Also, such atoms can be manipulated in optical fields to restrict metastable atom impact on the surface to a series of well defined lines or points obviating the need for a mask and offering the potential for massively parallel fabrication.¹²⁻¹⁹ To make use of these advantages, however, requires a reliable and reproducible procedure by which pattern transfer can be achieved. Two approaches that have been demonstrated involve using a self-assembled monolayer (SAM) as a resist^{11,20,21}, or allowing the metastable atoms to strike the surface in the presence of a hydrocarbon vapor.^{19,22} In these processes, the energy release that accompanies metastable atom deexcitation leads to damage of the SAM or formation of a durable carbonaceous deposit on the surface that has excellent resistance to a subsequent chemical etch.

Here we describe an alternate approach in which a hydrogen-passivated Si(100) surface is exposed behind a fine Ni grid to Ar(³P_{0,2}) metastable atoms in the presence of a small background pressure of oxygen. Ar(³P_{0,2}) deexcitation at the surface leads to formation of an oxide layer which is resistant to KOH etching to such an extent that feature depths $\gtrsim 20$ nm can be routinely realized. This technique has the advantage that it can be carried out in a clean, hydrocarbon-free vacuum environment, which results in good process control and excellent reproducibility. Furthermore, it is a process with inherent atomic-scale granularity, opening the possibility of atomic-scale lithography.

The present apparatus is shown schematically in Fig. 1. Argon atoms contained in a supersonic expansion are excited to the ³P_{0,2} metastable levels by electron impact excitation in a

dc discharge.²³ The supersonic nozzle is an aperture 150 μm in diameter laser-drilled in the end of a closed alumina tube. The aluminum skimmer, which has a 650 μm -diameter opening, is located ~ 6 mm downstream. To maximize metastable atom production, the discharge passes through the nozzle between a negatively biased tungsten cathode located inside the alumina tube and the grounded skimmer. Electron impact also leads to the formation of ions, photons and long-lived Rydberg states. Ions and Rydberg atoms are removed from the beam by application of a transverse electric field. To allow examination of possible effects due to the photons contained in the beam, a gas cell was also included in the beam line. With the introduction of an appropriate pressure of argon into the gas cell ($\sim 7 \times 10^{-2}$ Pa [5×10^{-4} Torr]) essentially all the metastable atoms can be scattered out of the beam while the photons continue through largely unattenuated. The $\text{Ar}(^3\text{P}_{0,2})$ flux provided by the source was estimated by measuring the secondary electron current ejected from a chemically-cleaned surface mounted in the final target chamber. The secondary electron ejection coefficient γ for such surfaces, however, depends markedly on their preparation and history. Nonetheless, previous work²⁴ suggests that it is reasonable to expect that the value of γ will lie in the range 0.05-0.20. Assuming a γ of 0.1, the measured secondary electron current would correspond to the production of 1×10^{15} $\text{Ar}(^3\text{P}_{0,2}) \text{ s}^{-1} \text{ sr}^{-1}$ by the source, yielding a dose rate of 2×10^{11} $\text{Ar}(^3\text{P}_{0,2}) \text{ s}^{-1} \text{ cm}^{-2}$ at the sample. This is sufficient to provide a "monolayer" surface exposure of 6.8×10^{14} atoms cm^{-2} in ~ 1 hr. Tests using the gas cell showed that only $\sim 10\%$ of the current leaving the surface was associated with photon impact.

The hydrogen passivated surfaces used here were prepared by initial cleaning in spectroscopic grade acetone and methanol with a deionized (DI) water rinse followed by 60 s immersion in 10% aqueous HF, a 30 s rinse in DI water and blow drying with N_2 . The samples were then placed in the target chamber which was immediately evacuated. Auger analysis of the passivated surfaces revealed strong Si features. A small C signal was also evident, but only trace amounts of O were detected. These findings are in agreement with earlier infrared studies^{25,26} which showed that the primary species present on a HF treated surface are (in order of decreasing

abundance) silicon di-, mono- and tri-hydride. X-ray photoelectron spectroscopy (XPS)^{26,27} and high resolution electron-energy-loss spectroscopy (HREELS)²⁷ investigations, however, revealed that small quantities of hydrocarbons can remain on a Si(100) surface following passivation in HF that can not be easily removed by baking²⁸. Indeed, neither the target nor the vacuum system was baked prior to metastable atom exposure because this led to an increase in C coverage on the surface, which was found to be detrimental to good oxide growth.

Patterning was studied by mounting the hydrogen passivated Si(100) target surfaces behind a Ni mesh that served as a mask (see Fig. 1). Target surfaces were exposed to the metastable atom beam in the presence of a small partial pressure ($\sim 3 \times 10^{-5}$ Pa [2×10^{-7} Torr]) of O₂. Tests revealed this resulted in the formation of the most uniform and etch resistant oxide layer. Following exposure, the vacuum system was brought up to atmospheric pressure by admitting O₂. After 20 min at 1 atm of O₂, the target was removed and immediately etched in a KOH bath. Although only a limited range of bath concentrations, bath temperatures and etching times was investigated, the best and most reproducible results were obtained by immersing the target in a room-temperature, stirred, 1M KOH solution for 90 s, followed by a 60 s rinse in DI water. The etched surfaces were examined using tapping mode atomic force microscopy (AFM).

A typical AFM image obtained after etching a hydrogen-passivated Si(100) surface exposed to $\sim 1 \times 10^{16}$ Ar(³P_{0,2}) atoms cm⁻² is shown in Fig. 2(a). A well defined grid pattern is evident with the unexposed areas etched to a depth of ~ 20 nm, as demonstrated by the averaged section in Fig. 2(b). This sizable feature depth indicates that the oxide layer formed by metastable atom impact in the presence of O₂ is robust and etch resistant. Its uniformity is demonstrated by the fact that the exposed areas remain relatively flat with no evidence of deep pitting. Tests showed that exposures as low as $\sim 2 \times 10^{15}$ Ar(³P_{0,2}) atoms cm⁻² were sufficient to allow good pattern transfer. For smaller exposures, however, pitting and increased roughness were noted in the exposed areas indicating that the oxide layer either had gaps in it where etching could begin or that it was too thin to adequately resist etching. Consequently only small feature depths could be achieved. Even after large Ar(³P_{0,2}) exposures, the oxide layer could be breached by extended or

more aggressive etching. Grid-like patterns were still discernible, but surface roughness was greatly increased. To check that oxide formation was associated with metastable atom rather than photon impact on the surface, tests were undertaken in which the metastable atoms in the beam were quenched using the gas cell, thereby allowing only the photons produced in the source to strike the surface. No pattern formation was observed after the same exposure time as used to obtain the image in Fig. 2. Furthermore, Auger analysis showed that metastable atom impact did not lead to a significant increase in the C coverage on the surface, demonstrating that build up of carbonaceous material is not occurring during metastable atom exposure.

The present work demonstrates that $\text{Ar}(^3\text{P}_{0,2})$ impact on a hydrogen-passivated $\text{Si}(100)$ surface can be used in the selective formation of a local oxide resist, although the exact mechanism by which this occurs remains unclear. One possibility is that the energy liberated by metastable atom deexcitation (~ 12 eV) leads directly to the breaking of Si-H bonds (which requires ~ 3.8 eV²⁹), leaving the exposed site vulnerable to subsequent attack by O_2 . Interestingly, the build up of a robust oxide layer might be enhanced through dissociation of physisorbed O_2 by metastable atom impact. (Gas phase studies of $\text{Ar}(^3\text{P}_{0,2})\text{-O}_2$ collisions have shown that metastable deexcitation is associated primarily with molecular dissociation and that the cross section for this process is large (35 \AA^2)³⁰) Earlier work has demonstrated that any process which leads to dissociation of physisorbed O_2 will enhance oxide growth.³¹ Indeed, an increase in the oxidation rate of $\text{Si}(100)$ by ambient O_2 has been observed when the surface is bombarded by 10 eV electrons.³² This effect is attributed to resonant dissociative electron attachment to physisorbed O_2 molecules.

Metastable impact without ambient O_2 present also resulted in pattern transfer. (Following exposure, however, the vacuum system was still brought to atmospheric pressure by admitting O_2 .) The oxide layers so formed were less reproducible and less etch resistant than those obtained with O_2 present during exposure. In the absence of O_2 the dominant constituent of the background gas is H_2O (partial pressure $\sim 4 \times 10^{-6}$ Pa [3×10^{-8} Torr]). Exposure of $\text{Si}(100)$ to

H₂O at 300 K is known to lead to formation of SiH and SiOH species^{33,34}, leaving oxygen on the surface. However, the exact mechanisms for this remain to be determined.

The use of metastable atoms to form oxide resists on hydrogen passivated Si surfaces provides a powerful new approach to performing nanoscale lithography. However, further work using different etchants and etching conditions, and with finer masks will be required to determine the maximum feature depths and spatial resolutions that can be achieved and to fully evaluate the capabilities of the technique.

This research was supported by the Division of Materials Science, Office of Basic Energy Sciences, U. S. Department of Energy and the Robert A. Welch Foundation.

References

1. N. Kramer, M. Niesten and C. Schönenberger, *Appl. Phys. Lett.* **67**, 2989 (1995).
2. S. Madsen, M. Müllenborn, K. Birkelund and F. Grey, *Appl. Phys. Lett.* **69**, 544 (1996).
3. M. Müllenborn, H. Dirac and J. W. Petersen, *Appl. Phys. Lett.* **66**, 3001 (1995).
4. R. E. Howard, H. G. Craighead, L. D. Jackel, P. M. Mankiewich and M. Feldman, *J. Vac. Sci. Technol. B* **1**, 1101 (1983).
5. E. S. Snow, P. M. Campbell and P. J. McMarr, *Appl. Phys. Lett.* **63**, 749 (1993).
6. N. Kramer, J. Jorritsam, H. Birk and C. Schönenberger, *J. Vac. Sci. Technol. B* **13**, 805 (1995).
7. J. W. Lyding, T. C. Shen, J. S. Hubacek, J. R. Tucker and G. C. Abeln, *Appl. Phys. Lett.* **64**, 2010 (1994).
8. P. M. Campbell, E. S. Snow and P. J. McMarr, *Surf. Sci.* **361**, 870 (1996).
9. H. C. Day and D. R. Allee, *Appl. Phys. Lett.* **62**, 2691 (1993).
10. J. A. Dagata, *et al*, *Appl. Phys. Lett.* **56**, 2001 (1990).
11. K. K. Berggren, *et al*, *Science* **269**, 1255 (1995).
12. G. Timp, *et al*, *Phys. Rev. Lett.* **69**, 1636 (1992).
13. J. J. McClelland, R. E. Scholten, E. C. Palm and R. J. Celotta, *Science* **262**, 877 (1993).
14. R. W. McGowan, D. M. Giltner and S. A. Lee, *Optics Lett.* **20**, 2535 (1995).
15. R. Gupta, J. J. McClelland, Z. J. Jabbour and R. J. Celotta, *Appl. Phys. Lett.* **67**, 1378 (1995).
16. V. Natarajan, R. E. Behringer and G. Timp, *Phys. Rev. A* **53**, 4381 (1996).
17. A. P. Chu, K. K. Berggren, K. S. Johnson and M. G. Prentiss, *Quantum and Semiclassical Optics* **8**, 521 (1996).
18. U. Drodofsky, *et al*, *Microelectronic Engineering* **35**, 285 (1997).
19. K. S. Johnson, *et al*, *Science* **280**, 1583 (1998).
20. S. Nowak, T. Pfau and J. Mlynek, *Appl. Phys. B* **63**, 203 (1996).

21. S. B. Hill, *et al*, (manuscript in preparation)
22. K. S. Johnson, *et al*, *Appl. Phys. Lett.* **69**, 2773 (1996).
23. D. W. Fahey, W. F. Parks and L. D. Schearer, *J. Phys E: Sci. Instrum.* **13**, 381 (1980).
24. S. Schohl, H. A. J. Meijer, M. Ruf and H. Hotop, *Meas. Sci. Tech.* **3**, 544 (1992).
25. Y. J. Chabal, G. S. Higashi and K. Raghavachari, *J. Vac. Sci. Technol. A* **7**, 2104 (1989).
26. L. Zazzera and J. F. Evans, *J. Vac. Sci. Technol. A* **11**, 934 (1993).
27. M. Grundner and H. Jacob, *Appl. Phys. A* **39**, 73 (1985).
28. H. Hanbücken, H. Neddermayer and J. R. Vanables, *Surf. Sci.* **137**, L92 (1984).
29. H. N. Waltenburg and J. T. Yates, *Chem. Rev.* **95**, (1995).
30. D. Rickey and J. Krenos, *J. Chem. Phys.* **106**, 3135 (1996).
31. T. Engel, *Surf. Sci. Rep.* **18**, 91 (1993).
32. J. Xu, W. J. Choyke and J. T. Yates, *J. Appl. Phys.* **82**, 6289 (1997).
33. M. Niwano, T. Miura, Y. Kimura, R. Tajima and N. Miyamoto, *J. Appl. Phys.* **79**, 3708 (1996).
34. M. K. Weldon, B. B. Stefanov, K. Raghavachari and Y. J. Chabal, *Phys. Rev. Lett.* **79**, 2851 (1997).

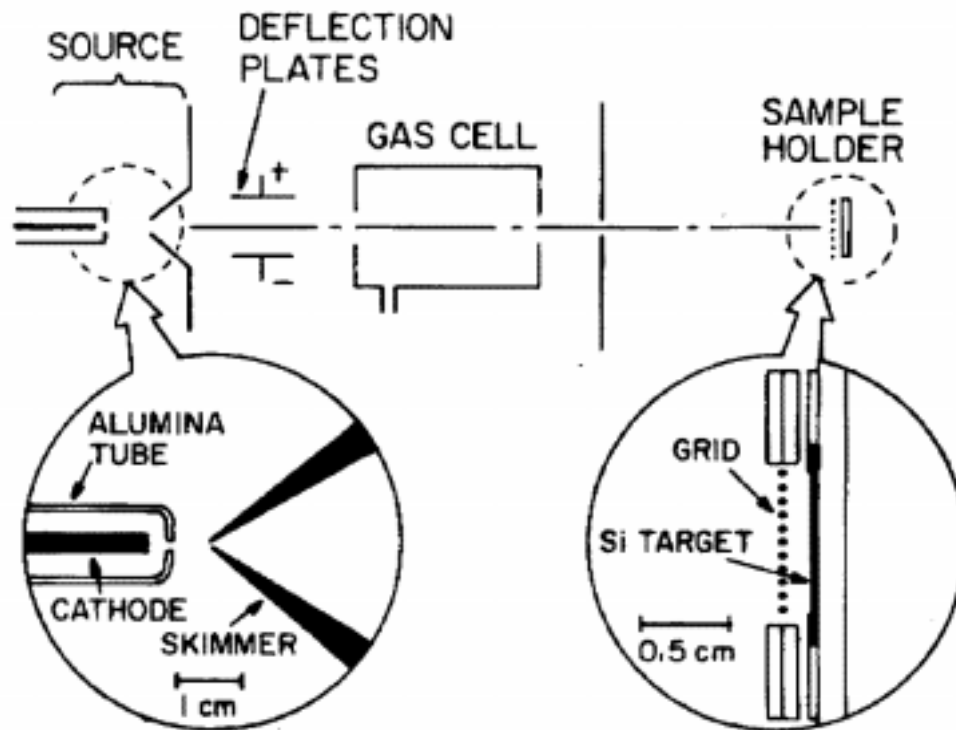


Fig. 1. Schematic of the apparatus. A beam of metastable Ar atoms, produced in a DC discharge, strikes a hydrogen-passivated Si wafer. Deflector plates remove ions and Rydberg atoms from the beam, and a gas cell provides a means to quench the metastable atoms without otherwise affecting the beam. The beam is patterned before striking the wafer by passing through a square Ni grid with $12.7\ \mu\text{m}$ pitch ($5.1\ \mu\text{m}$ wires and $7.6\ \mu\text{m}$ spaces).

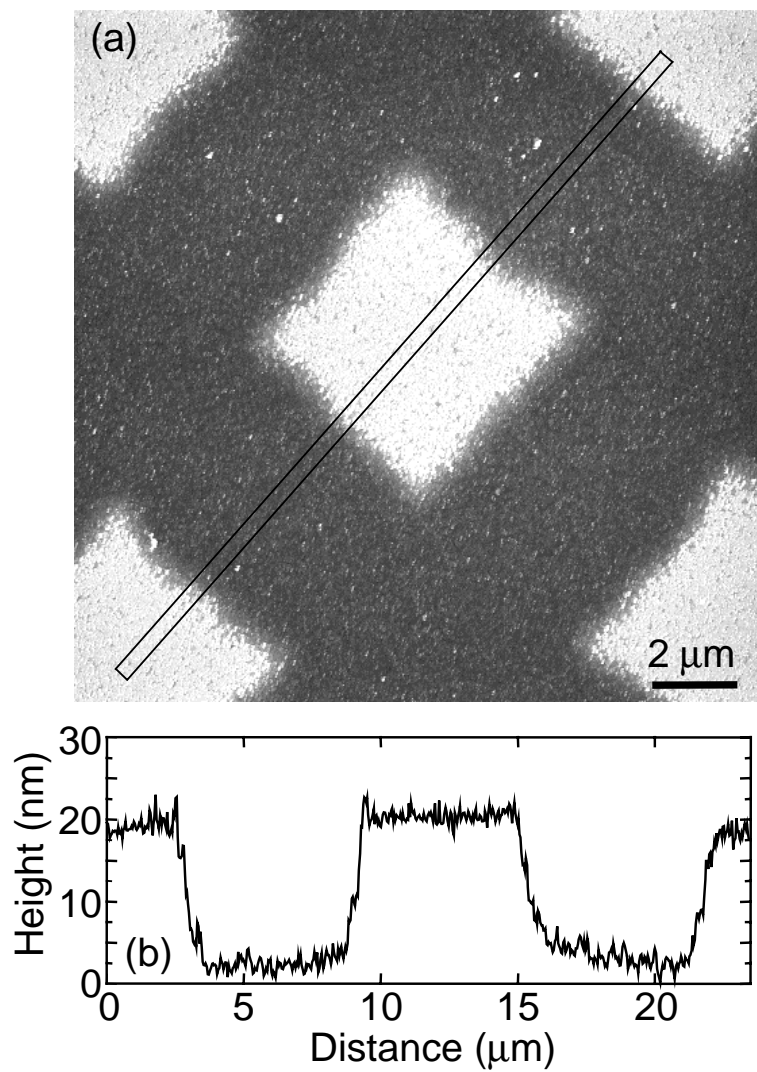


Fig. 2. (a) Tapping mode AFM image of hydrogen-passivated Si(100) following exposure to $\sim 1 \times 10^{16}$ Ar($^3\text{P}_{0,2}$) atoms cm^{-2} in the presence of $\sim 3 \times 10^{-5}$ Pa (2×10^{-7} Torr) partial pressure of O_2 and KOH etch. (b) Section from (a) to show feature depths averaged over region indicated in box.